

## Supporting Information

### Characterization of Glycerophospholipids at Multiple Isomer Levels via Mn(II)-Catalyzed Epoxidation

Xi Chen,<sup>a</sup> Shuli Tang,<sup>a</sup> Dallas Freitas,<sup>a</sup> Erin Hirtzel,<sup>a</sup> Heyong Cheng,<sup>a</sup> Xin Yan<sup>\*a</sup>

<sup>a</sup> Department of Chemistry, Texas A&M University, 580 Ross St., College Station, TX 77845 (USA)

#### Table of content

- S1. Condition optimization of Mn-catalyzed lipid C=C bond epoxidation
- S2. Analysis of diagnostic ions of C=C bond positions upon HCD
- S3. Identification of C=C bond-positional isomers in various lipid classes
- S4. Analysis of Mn adducts with various lipid classes
- S5. Mn-catalyzed epoxidation for C=C bond- and *sn*-positional isomer identification
- S6. Investigation of divalent metal ions in the formation of epoxides and metal adducts for C=C bond and *sn*-position determination
- S7. Discussion of oxidants and ligands used in Mn<sup>2+</sup> catalyzed epoxidation
- S8. Limit of detection
- S9. PLA<sub>2</sub> digestion experiment
- S10. Relative quantification of *sn*-positional isomers
- S11. Lipid isomer identification using lipid extract from egg yolk
- S12. Comparison of Mn<sup>2+</sup> catalyzed epoxidation to other methods for lipid isomer identification

## S1. Condition optimization of Mn-catalyzed lipid C=C bond epoxidation

### S1.1. PAA<sub>M</sub> and PAA as oxidation reagents for C=C bond epoxidation

Previous work by Moretti *et al*<sup>1</sup> recommended using 1.1 equiv. of modified PAA (PAA<sub>M</sub>), 0.4 mol% of Mn(CF<sub>3</sub>SO<sub>3</sub>)<sub>2</sub>, and 2 mol% of picolinic acid for achieving the best yields of epoxidation in ACN. When PAA<sub>M</sub> was used as an oxidant, 1.1 equiv. of PAA<sub>M</sub> could give a moderate epoxidation yield. However, additional acids such as formic acid were needed for protonation.

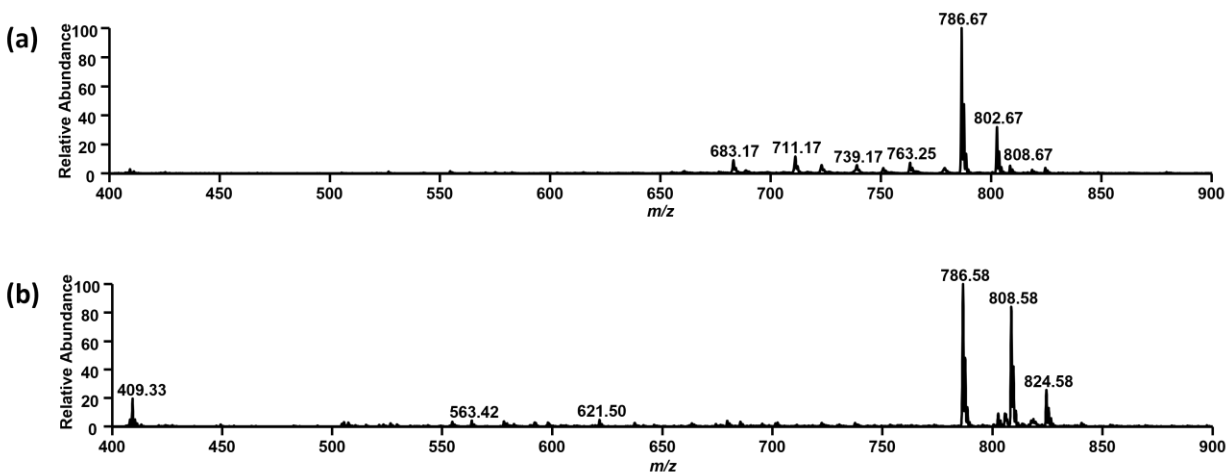


**Figure S1.** Mass spectra after epoxidation of PC 18:1(9)/18:1(9) of 50  $\mu$ M using PAA<sub>M</sub> (55  $\mu$ M, 1.1 equiv.), Mn(CF<sub>3</sub>SO<sub>3</sub>)<sub>2</sub> (0.2  $\mu$ M), picolinic acid (1  $\mu$ M) in ACN (a) with 1% formic acid and (b) without any additional acid.

The epoxidation products using PAA were less than those using PAA<sub>M</sub>. Epoxides could not be seen when 1.1 equiv. of PAA was applied. As the concentration of PAA and catalyst increased, more and more epoxides could be obtained and the two C=C bonds in PC 18:1(9)/18:1(9) were both epoxidized. Excessive reagents can lead to over-epoxidized products, which appeared at  $m/z$  834 (+48 Da), and  $m/z$  850 (+64 Da). The amount of PAA was found to be 3.3 equiv. to 5.5 equiv. for good epoxidation yields without extensive side products. No additional formic acid was needed, and the formation of alkaline metal ion adducts could be avoided.

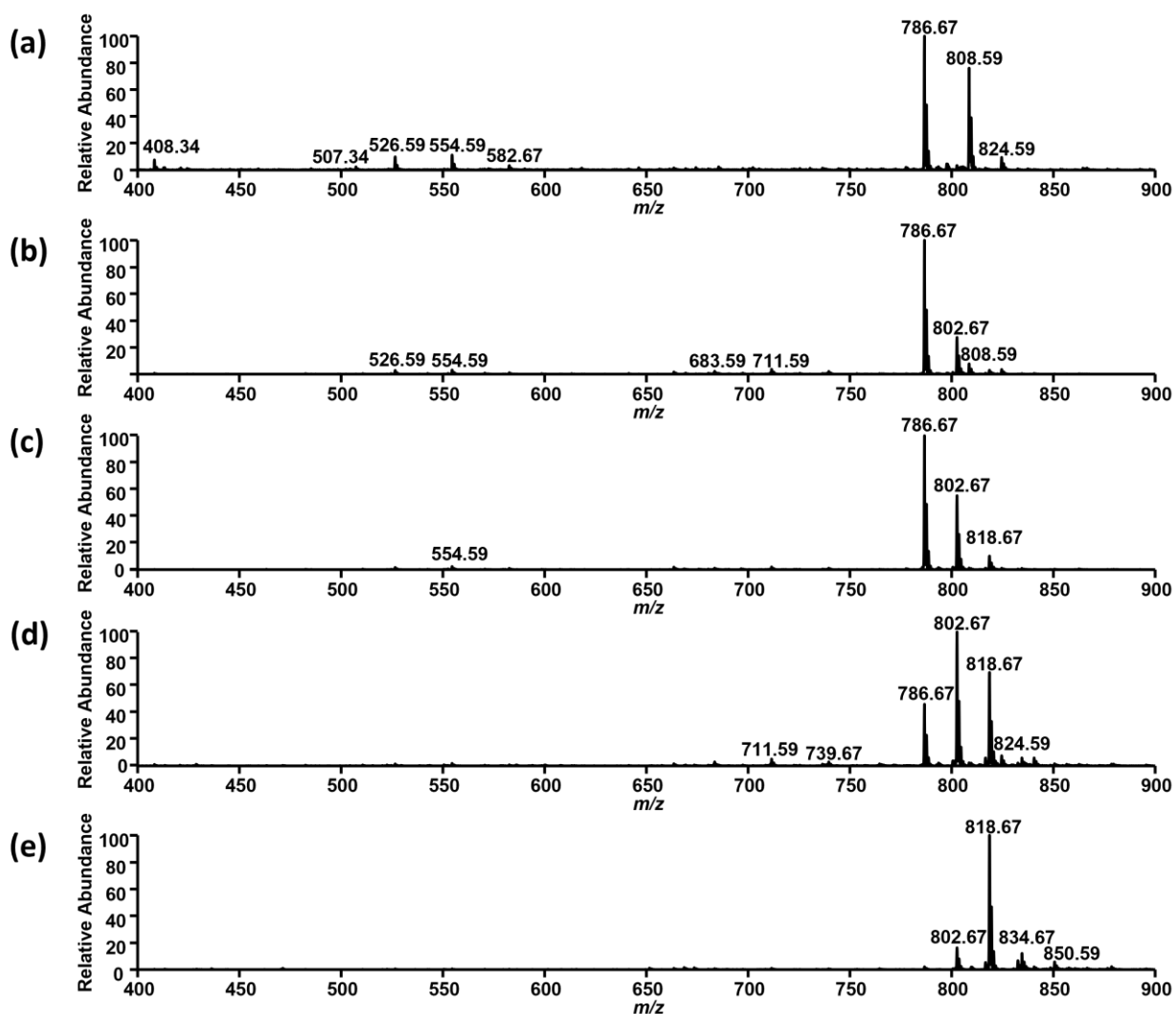


**Figure S2.** Mass spectra after epoxidation of PC 18:1(9)/18:1(9) (50  $\mu\text{M}$ ) using various concentrations of PAA and catalyst in ACN. (a) PAA 55  $\mu\text{M}$  (1.1 equiv.),  $\text{Mn}(\text{CF}_3\text{SO}_3)_2$  0.2  $\mu\text{M}$  and picolinic acid 1  $\mu\text{M}$ ; (b) PAA 110  $\mu\text{M}$  (2.2 equiv.),  $\text{Mn}(\text{CF}_3\text{SO}_3)_2$  0.4  $\mu\text{M}$  and picolinic acid 2  $\mu\text{M}$ ; (c) PAA 165  $\mu\text{M}$  (3.3 equiv.),  $\text{Mn}(\text{CF}_3\text{SO}_3)_2$  0.6  $\mu\text{M}$  and picolinic acid 3  $\mu\text{M}$ ; (d) PAA 275  $\mu\text{M}$  (5.5 equiv.),  $\text{Mn}(\text{CF}_3\text{SO}_3)_2$  1  $\mu\text{M}$  and picolinic acid 5  $\mu\text{M}$ ; (e) PAA 550  $\mu\text{M}$  (11 equiv.),  $\text{Mn}(\text{CF}_3\text{SO}_3)_2$  2  $\mu\text{M}$  and picolinic acid 10  $\mu\text{M}$ .

### S1.2. Mn(II) as a catalyst for C=C bond epoxidation

$\text{Mn}^{2+}$  catalysts are essential as epoxidation yields were very low with solely PAA or  $\text{PAA}_M$  after a reaction time of 10 min. With  $\text{Mn}^{2+}$  catalysts, epoxidation was triggered immediately. Mn(II) coordinated with picolinic acid and formed the

complex for catalysis. Epoxides were not observed when mixing PAA and lipid alone (Fig S3(a)). After adding Mn(II) salts and picolinic acid, epoxidation occurred.

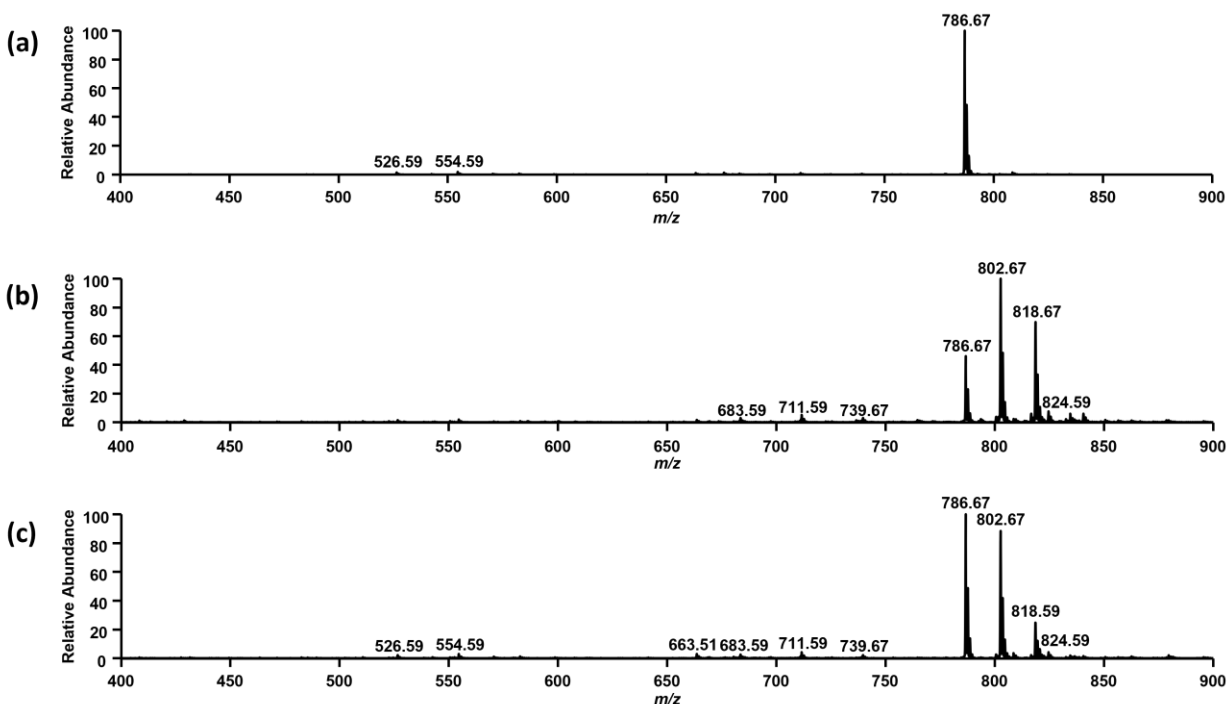


**Figure S3.** Mass spectra showing the effects of catalysts on epoxidation using (a) PC 18:1(9)/18:1(9) (50  $\mu$ M), and PAA (275  $\mu$ M, 5.5 equiv.); (b) PC 18:1(9)/18:1(9) (50  $\mu$ M), PAA (275  $\mu$ M, 5.5 equiv.), and Mn(CF<sub>3</sub>SO<sub>3</sub>)<sub>2</sub> (1  $\mu$ M), and picolinic acid (5  $\mu$ M); (c) PC 18:1(9)/18:1(9) (50  $\mu$ M), PAA (275  $\mu$ M, 5.5 equiv.), MnCl<sub>2</sub> (1  $\mu$ M), and picolinic acid (5  $\mu$ M) in ACN.

### S1.3. Investigation of reaction solvent

Several solvent systems have been investigated. The reaction happened readily in ACN, CHCl<sub>3</sub>, and H<sub>2</sub>O, while showing less or no activity in DMF, EtOAc, MeOH, and THF.

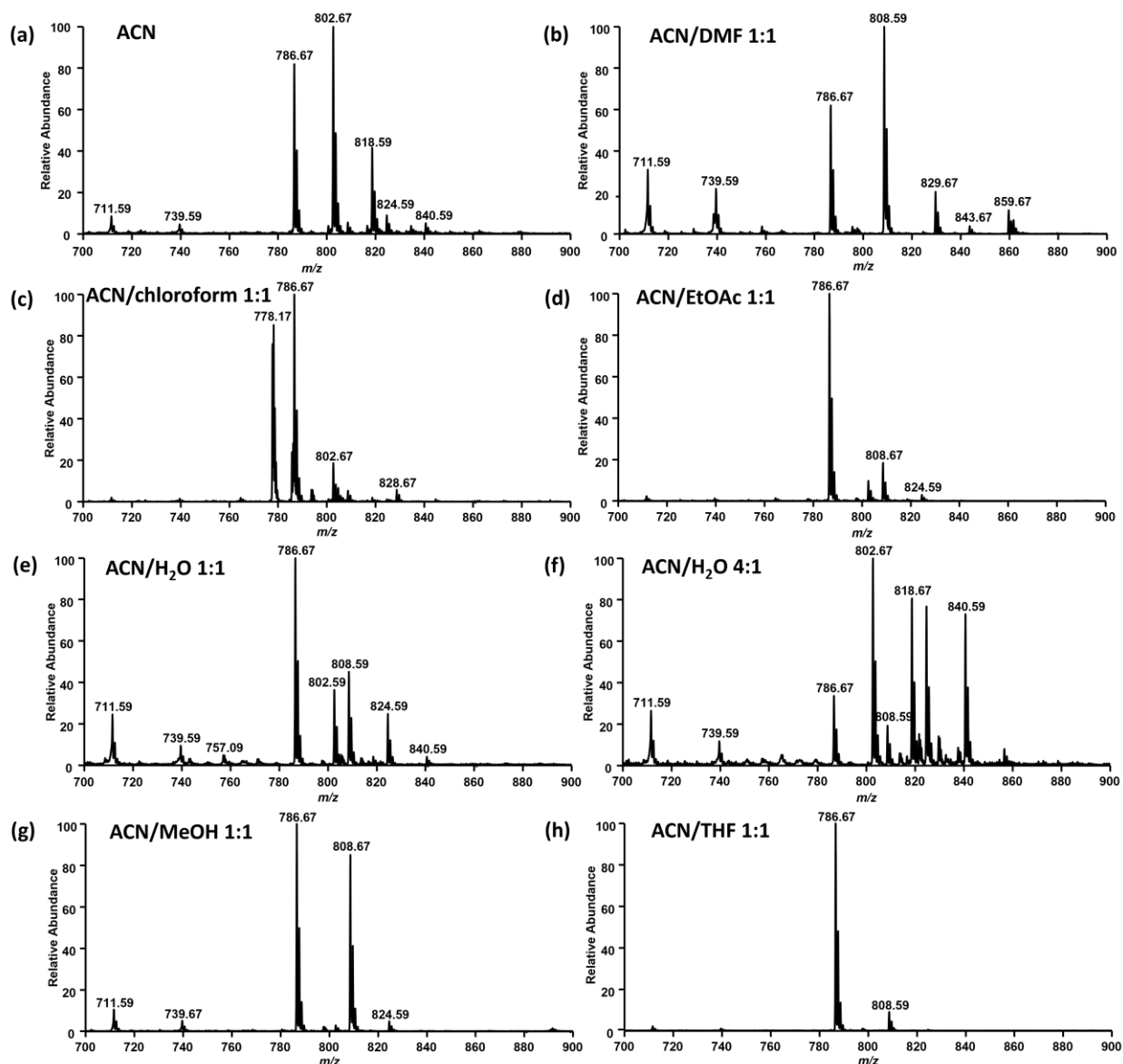


**Figure S4.** Mass spectra after epoxidation of PC 18:1(9)/18:1(9) (50  $\mu$ M) using PAA (275  $\mu$ M, 5.5 equiv.),  $\text{Mn}(\text{CF}_3\text{SO}_3)_2$  (1  $\mu$ M), and picolinic acid (5  $\mu$ M) in various solvent systems.

**Table S1.** Summary of C=C bond epoxidation in various solvent systems. Conversion rates were calculated as the sum intensities of ions at  $m/z$  802 and 818 divided by the sum intensities of ions at  $m/z$  786,  $m/z$  802, and  $m/z$  818.

Solvent	Intensity of $m/z$ 786	Intensity of $m/z$ 802	Intensity of $m/z$ 818	Conversion rate
ACN	$2.70 \times 10^6$	$3.29 \times 10^6$	$1.37 \times 10^5$	63.3%
ACN/DMF 1:1	$3.37 \times 10^5$	$2.95 \times 10^3$	$2.60 \times 10^3$	1.62%
ACN/chloroform 1:1	$2.88 \times 10^6$	$5.44 \times 10^5$	$6.27 \times 10^4$	17.4%
ACN/EtOAc 1:1	$1.53 \times 10^6$	$1.28 \times 10^5$	$1.13 \times 10^4$	8.34%
ACN/H <sub>2</sub> O 1:1	$5.13 \times 10^5$	$1.90 \times 10^5$	$2.23 \times 10^4$	29.3%
ACN/H <sub>2</sub> O 4:1	$7.37 \times 10^5$	$2.18 \times 10^6$	$1.76 \times 10^6$	84.2%
ACN/MeOH 1:1	$1.87 \times 10^6$	$5.62 \times 10^4$	$3.31 \times 10^3$	3.08%
ACN/THF 1:1	$3.58 \times 10^6$	$7.32 \times 10^3$	$6.77 \times 10^3$	3.94%

#### S1.4. Reaction monitoring of C=C bond epoxidation

Reaction monitoring was conducted with PC 18:1(9)/18:1(9) (50  $\mu$ M), PAA (165  $\mu$ M), Mn(CF<sub>3</sub>SO<sub>3</sub>)<sub>2</sub> (0.6  $\mu$ M) and picolinic acid (3  $\mu$ M) in ACN. After adding all the reagents, the solution was immediately loaded into a nanoESI emitter, and the mass spectra and ion chromatograms were recorded. Native lipid ( $m/z$  786), mono-epoxidized lipid ( $m/z$  802), and di-epoxidized lipid ( $m/z$  818) were observed upon the application of spray voltage. The intensity of ions at  $m/z$  786 decreased as the intensity of ions at  $m/z$  818 increased. The intensity of ions at  $m/z$  802 remained stable after about 3 minutes.

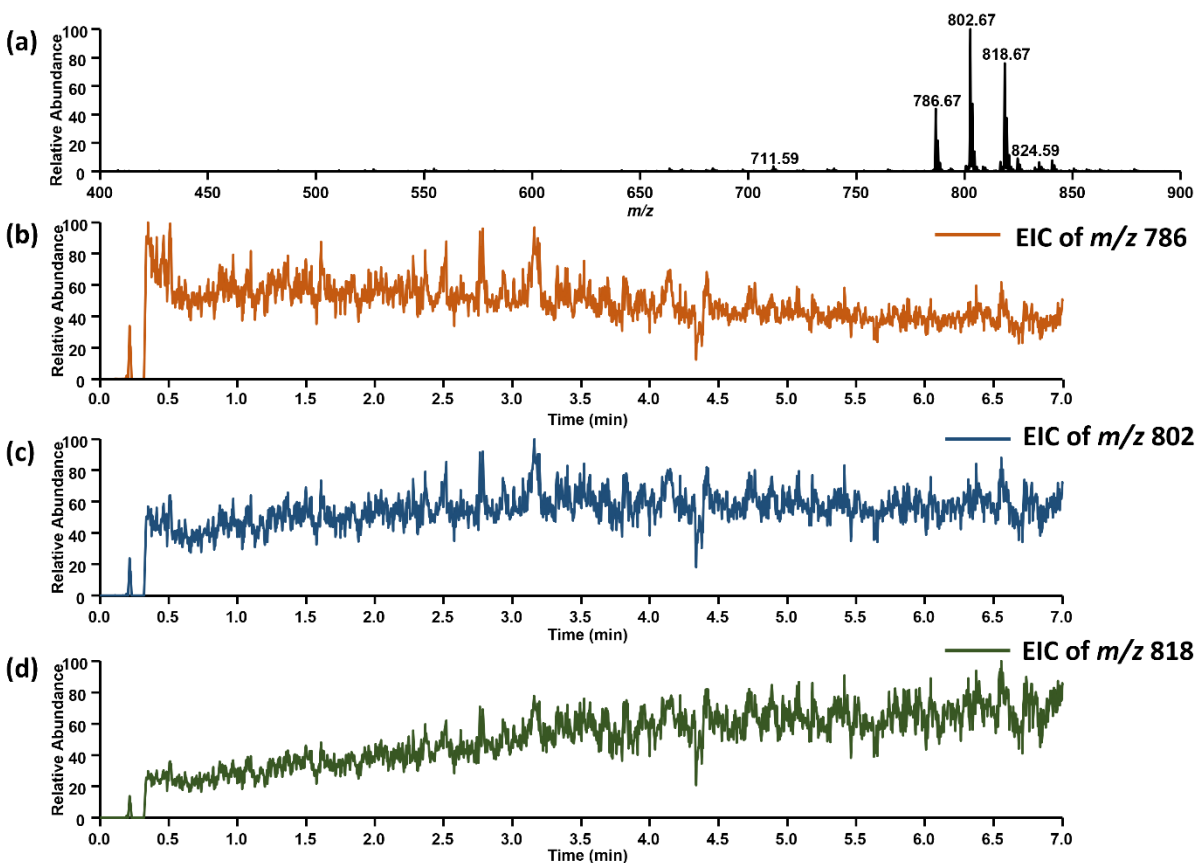


**Figure S5.** Extracted ion chromatograms (EIC) showing reaction monitoring of double bond epoxidation. (a) Averaged mass spectrum at 3-4 minutes after applying the spray voltage; (b), (c), and (d) EICs of ions at  $m/z$  786, 802, and 818, respectively.

## S2. Analysis of diagnostic ions of $C=C$ bond positions upon HCD

MS/MS experiment using HCD was also conducted; however, few diagnostic ions of  $C=C$  bond positions were observed in HCD spectra. This was consistent with previous studies.<sup>2, 3</sup>

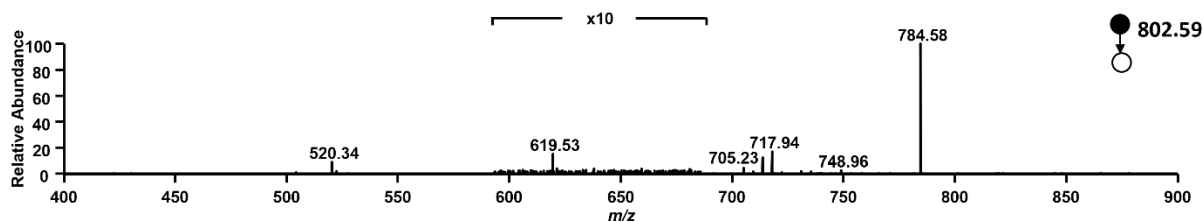


**Figure S6.** HCD spectrum of the epoxidized lipid of PC 18:1(9)/18:1(9) at  $m/z$  802.

### S3. Identification of C=C bond-positional isomers in various lipid classes

#### S3.1. Identification of C=C bond-positional isomers of fatty acids 18:1(9) and 20:4 (5,8,11,14)

Fatty acids 18:1(9) and 20:4 (5,8,11,14) were epoxidized successfully with Mn(II)/picolinic acid/PAA, and the diagnostic ions were observed to locate the C=C bonds. They had higher reaction yields than PCs, showing higher diagnostic ion intensities.

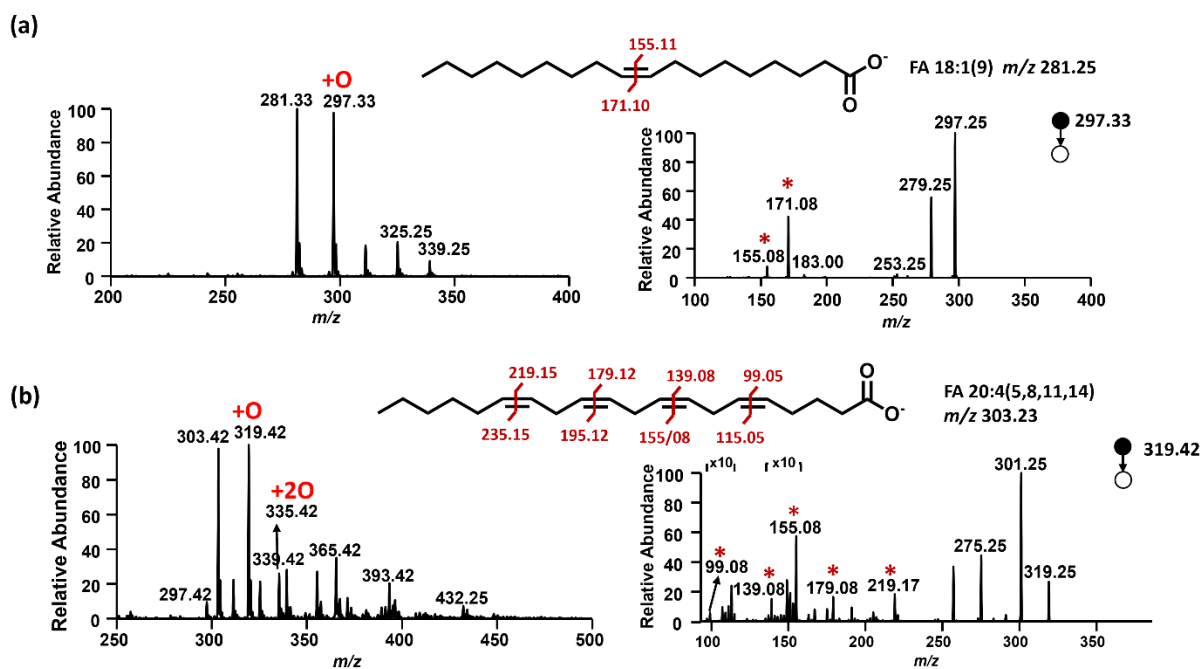


**Figure S7.** Mass spectra after epoxidation of (a) FA 18:1(9) and (b) FA 20:4(5,8,11,14). The reaction was conducted with FA (50  $\mu$ M), PAA<sub>M</sub> (55  $\mu$ M), MnCl<sub>2</sub> (1  $\mu$ M), and picolinic acid (5  $\mu$ M).

#### S3.2. Identification of C=C bond-positional isomers of PS 18:1(9)/18:1(9) and PG 18:1(9)/18:1(9)

Phospholipids other than PCs such as PS and PG were analyzed as well, both displaying epoxidation products in the mass spectra. These two lipids were detected in negative ion mode and the diagnostic ions were found in the CID-MS<sup>3</sup> spectra from the cleavage of epoxidized 18:1(9) chain in lipids.

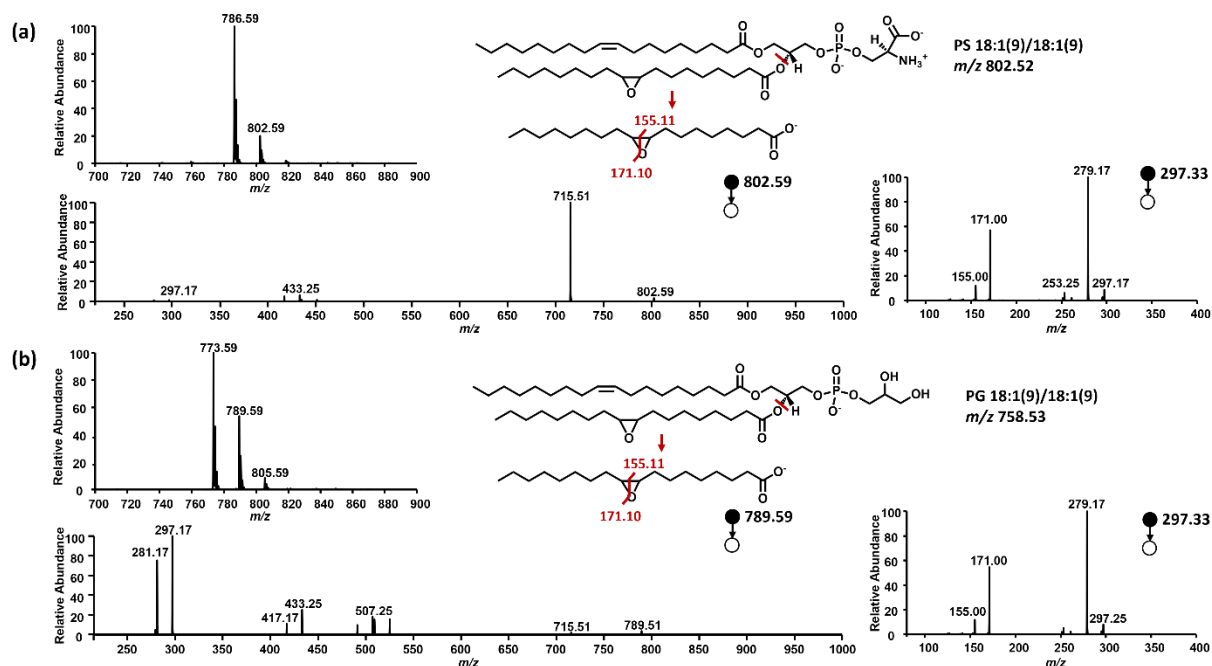


**Figure S8.** Mass spectra after epoxidation of (a) PS 18:1(9)/18:1(9) and (b) PG 18:1(9)/18:1(9). The reaction was conducted with lipid (50  $\mu$ M), PAA (275  $\mu$ M),  $\text{Mn}(\text{CF}_3\text{SO}_3)_2$  (1  $\mu$ M), and picolinic acid (5  $\mu$ M).

#### S4. Analysis of Mn adducts with various lipid classes

Fatty acids formed positively charged Mn-lipid adducts that provide more fragments upon CID for structural analysis. For example, in negative ion mode oleic acid mainly showed  $\text{H}_2\text{O}$  loss peaks and  $\text{CO}_2$  loss peaks; however, in positive ion mode,  $[\text{oleic acid} + \text{Mn}]^+$  species showed more fragments, most coming from the charge-remote fragmentation at each carbon-carbon bond, as reported by Yoo *et al.*<sup>4</sup> Fragments from  $[\text{epoxidized oleic acid} + \text{Mn}]^+$  gave an obvious peak at  $m/z$  210.00, which was assigned to the cleavage of the oxirane ring.  $\text{Mn}^{2+}$  and phospholipids other than PC and PE formed singly-charged Mn-lipid adducts. These singly-charged adducts released  $[\text{M} + \text{FAsn} - 2]^+$  and  $[\text{M} + \text{lipid} - \text{FAsn} - 2]^+$ , but it is not clear that this observation was attributed to the affinity of Mn to fatty acyl chain at *sn*-2 or to the C=C bond on the fatty acyl chain. PE lipids showed doubly charged adducts as well, but the fragmentation pattern was different from that of PCs and the feasibility of  $[\text{M} + \text{FA}]^+$  ions for *sn*-positional isomer identification still needs further validation. Therefore, in this study, *sn*-positional isomer identification via  $\text{Mn}^{2+}$  is focused on PCs.

### S4.1. Fatty acid-Mn adduct

Oleic acid (FA 18:1(9)) was found to bind with Mn ion and form a singly charged oleic acid-Mn adduct, which allowed oleic acid to be detected in positive ion mode. Upon CID, most fragments were  $C_xH_{2x-4}O_2+Mn$ ,  $C_xH_{2x-6}O_2+Mn$ , or other species formed via C-C bond or C-H bond cleavage. Epoxidized oleic acid was observed in positive ion mode with the addition of Mn ions as well, and its tandem mass spectrum contained one fragment with high intensity at  $m/z$  210, which resulted from the cleavage at the C=C bond position.

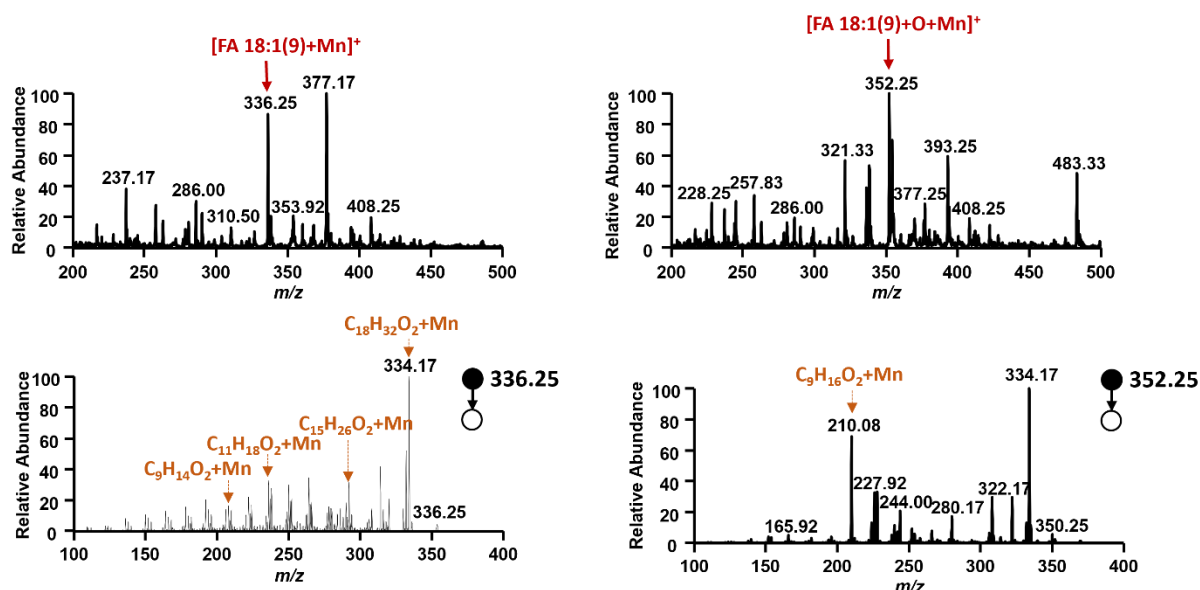


**Figure S9.** Mass spectra showing Mn adducts with (a) oleic acid and (b) epoxidized oleic acid. Oleic acid (50  $\mu$ M) and  $Mn(CF_3SO_3)_2$  (100  $\mu$ M) were mixed in ACN/ $H_2O$  4:1 solution. For epoxidation, additional PAA (275  $\mu$ M), and picolinic acid (5  $\mu$ M) were added.

### S4.2. PE-Mn adduct

PE 16:0/18:1(9) was used in the experiment. The doubly-charged Mn adduct of PE16:0/18:1(9) was formed but the intensity was much lower than the adducts with PCs. Moreover, the fragmentation pattern of this adduct was different from those with PCs.  $[FA\ 18:1(9) + Mn]^+$  was observed while the Mn adduct with the other fatty acyl chain FA 16:0 was missing after fragmentation. It was not clear whether this was due to selective binding of Mn with fatty acyl chain at the *sn*-2 position or with unsaturated fatty acyl chain. The potential of applying PE-Mn adduct to *sn*-positional isomer identification needs further investigation.

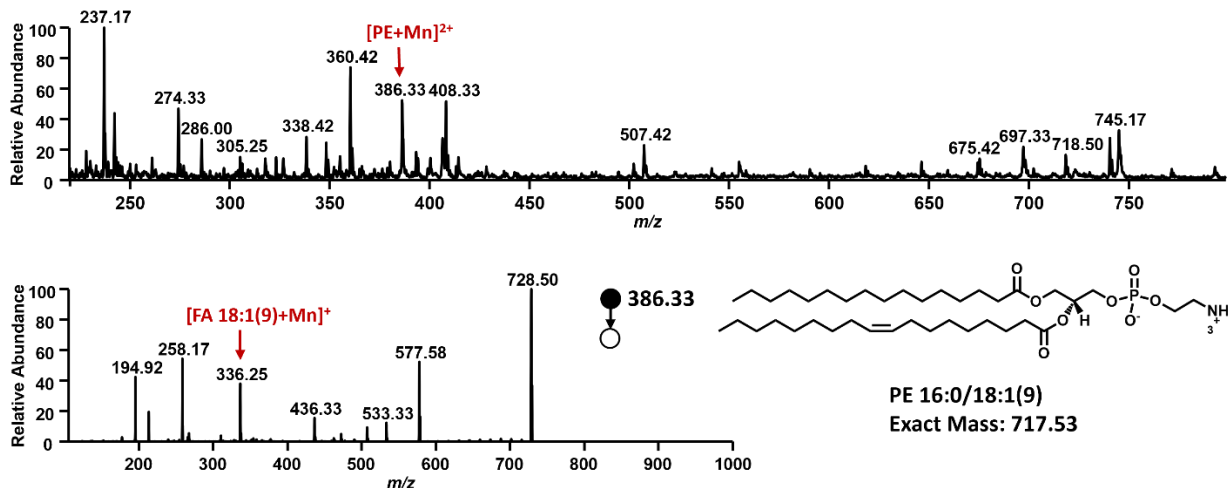


**Figure S10.** Mass spectra showing Mn adducts with PE 16:0/18:1(9) and its tandem mass spectrum. PE 16:0/18:1(9) (50  $\mu$ M) and Mn(CF<sub>3</sub>SO<sub>3</sub>)<sub>2</sub> (100  $\mu$ M) were mixed in ACN/H<sub>2</sub>O 4:1 solution.

### S4.3. PG-Mn adduct

PG 16:0/18:1(9) were found to bind with the Mn ion and form singly-charged ions due to the negative charge of the lipid headgroup. Upon CID, many fragments were generated, including [FA 18:1(9)+Mn]<sup>+</sup>; however, no diagnostic ions related to *sn* positions were observed.

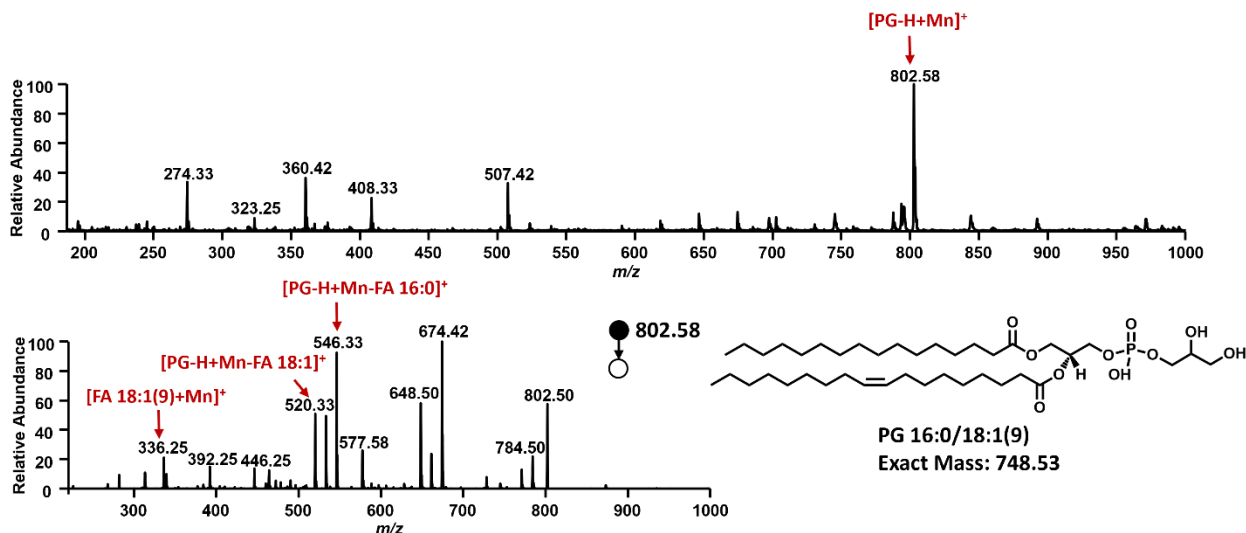


**Figure S11.** Mass spectra showing Mn adducts with PG 16:0/18:1(9) and its tandem mass spectrum. PG 16:0/18:1(9) (50  $\mu$ M) and Mn(CF<sub>3</sub>SO<sub>3</sub>)<sub>2</sub> (100  $\mu$ M) were mixed in ACN/H<sub>2</sub>O 4:1 solution.

### S4.4. PS-Mn adduct

PS 18:1(9)/18:1(9) were used to bind with Mn(II). This lipid formed a singly-charged lipid-Mn adduct, but its fragments were simple, consisting mainly of headgroup loss and fatty acyl chain loss ions.

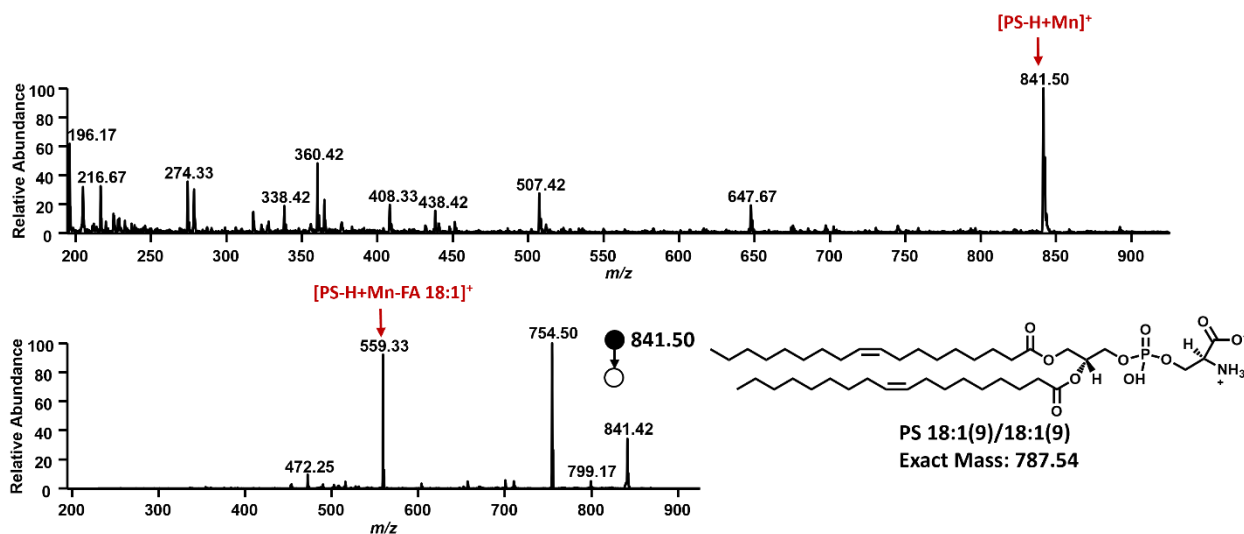


**Figure S12.** Mass spectra showing Mn adducts with PS 18:1(9)/18:1(9) and its tandem mass spectrum. PS 18:1(9)/18:1(9) (50  $\mu$ M) and Mn(CF<sub>3</sub>SO<sub>3</sub>)<sub>2</sub> (100  $\mu$ M) were mixed in ACN/H<sub>2</sub>O 4:1 solution.

## S5. Mn-catalyzed epoxidation for C=C bond- and *sn*-positional isomer identification

### S5.1. C=C bond- and *sn*-positional isomer identification of PC 18:1(9)/18:1(9) and PC 18:1(6)/18:1(6)

PC 18:1(9)/18:1(9) and PC 18:1(6)/18:1(6) were studied. Ions of epoxide  $m/z$  802 and Mn-lipid adduct at  $m/z$  420 were found. Upon CID, they produced the corresponding diagnostic ions.

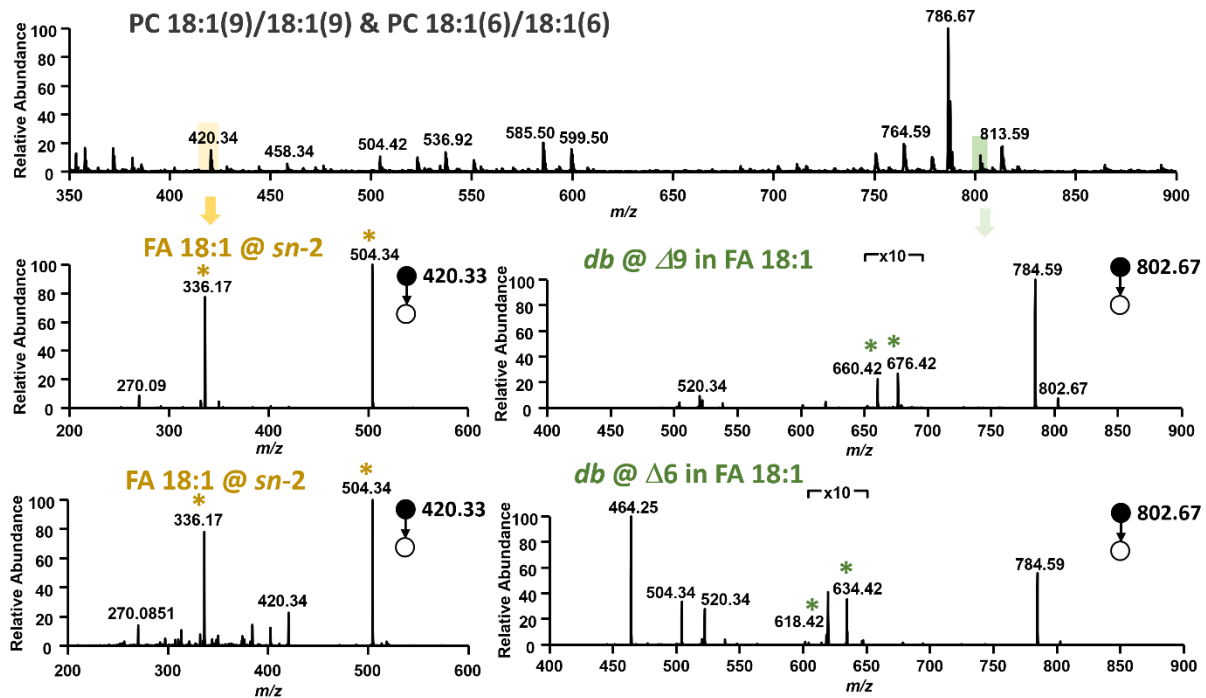


**Figure S13.** Mass spectra after Mn-catalyzed epoxidation for lipid identification of PC 18:1(9)/18:1(9) and PC 18:1(6)/18:1(6). PC 18:1(9)/18:1(9) or PC 18:1(6)/18:1(6) (50  $\mu$ M), PAA (275  $\mu$ M), Mn(CF<sub>3</sub>SO<sub>3</sub>)<sub>2</sub> (100  $\mu$ M) and picolinic acid (1  $\mu$ M) were mixed in ACN.

## S5.2. Lipid isomer identification with Mn-epoxidized lipid adduct

Doubly-charged Mn-epoxidized lipid adducts have also been detected in Mn-catalyzed epoxidation. However, an obvious distinct fragmentation pattern has not been found in CID.

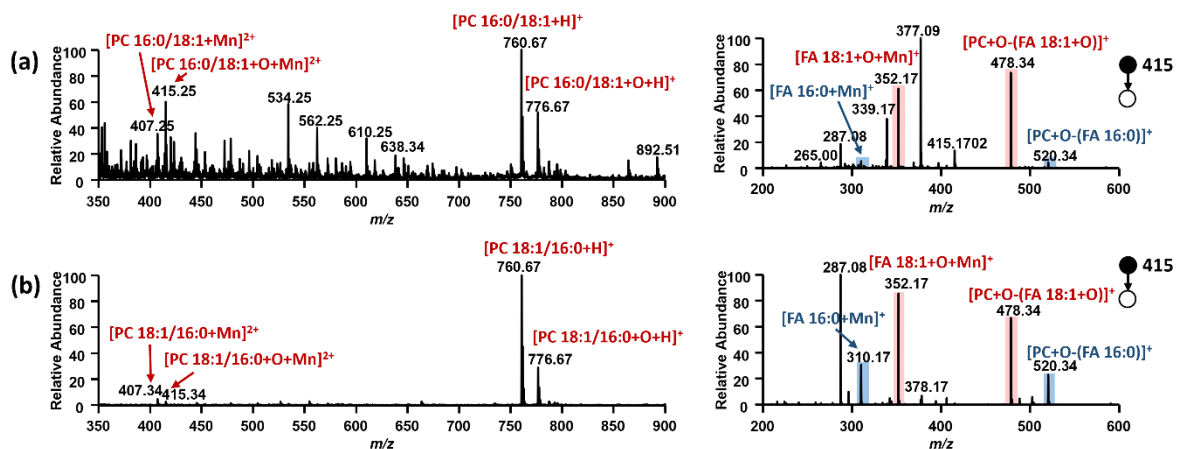


**Figure S14.** Full mass spectra and tandem mass spectra of Mn-epoxidized lipid adduct of (a) PC 16:0/18:1 and (b) PC 18:1/16:0 under Mn-catalyzed epoxidation. PC 16:0/18:1 or PC 18:1/16:0 (50  $\mu\text{M}$ ), PAA (275  $\mu\text{M}$ ),  $\text{Mn}(\text{CF}_3\text{SO}_3)_2$  (100  $\mu\text{M}$ ) and picolinic acid (1  $\mu\text{M}$ ) were mixed in ACN.

## **S6. Investigation of divalent metal ions in the formation of epoxides and metal adducts for C=C bond and *sn*-position determination**

Divalent metal ions from  $\text{MnCl}_2$ ,  $\text{CuCl}_2$ ,  $\text{FeCl}_2$ , and  $\text{CoCl}_2$  were used to catalyze lipid epoxidation by PAA and picolinic acid and form metal adducts for C=C bond and *sn*-position determination. The full mass spectra and tandem mass spectra after metal adduct formation and epoxidation catalyzed by  $\text{MnCl}_2$ ,  $\text{CuCl}_2$ ,  $\text{FeCl}_2$ , and  $\text{CoCl}_2$  were shown in Figure S15. Lipid metal adducts and epoxides were formed in all reactions catalyzed by these metals but to different extents and not all of their fragmentations could be used for isomer identification. Co(II) showed the best catalytic activity as PC 16:0/18:1 was completely converted to lipid epoxide, but side products were formed at high intensities. Cu(II) reaction produced the Cu-lipid adduct, but its fragmentation did not produce ions for *sn*-positional isomer determination. Fe(II) catalyzed reaction produced the lowest abundance of lipid epoxide. Mn(II) catalyzed reaction had moderate epoxidation yield and generated the highest abundance of metal-lipid adducts. Their fragments could be used to locate C=C bond and *sn*-positions. Importantly, it produced the least amount of side products such as PC-Cl adduct at  $m/z$  794. Therefore, Mn(II) was chosen for this work.

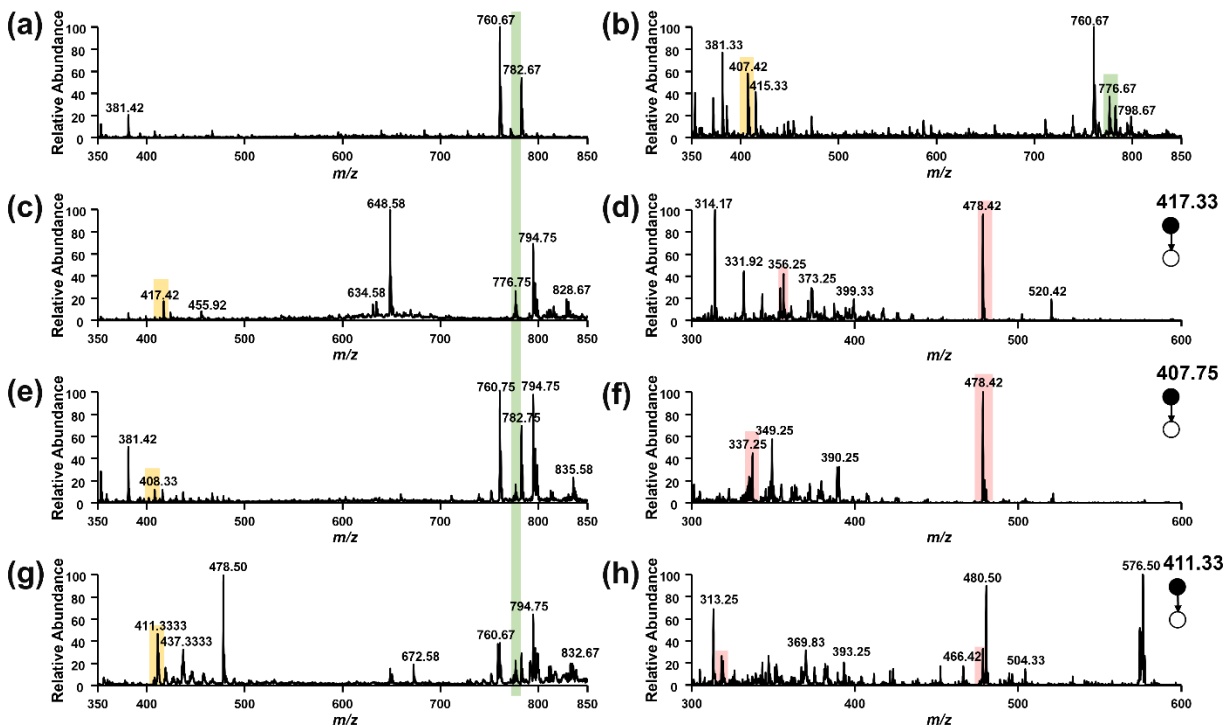


**Figure S15.** Mass spectra after divalent metal-catalyzed epoxidation of 50  $\mu\text{M}$  PC 16:0/18:1(9) using 100  $\mu\text{M}$  chloride salts of different divalent metals, 1  $\mu\text{M}$  picolinic acid, and 275  $\mu\text{M}$  PAA. (a) Full mass spectrum of reaction solution without metal ion. Full mass spectrum after (b) Mn(II)-, (c) Co(II)-, (e) Fe(II)- and (g) Cu(II)- catalyzed epoxidation. Tandem mass spectra of (d) Co(II)-, (f) Fe(II)- and (h) Cu(II)- lipid adduct. Here, as native lipids ( $m/z$  760) were absent from Co(II)-catalyzed epoxidation, Co(II)-lipid adduct was chosen as the adduct of epoxidized PC ( $m/z$  417.3) instead of native PC ( $m/z$  409.3).

## S7. Discussion of oxidants and ligands used in $\text{Mn}^{2+}$ catalyzed epoxidation

Peracetic acid (PAA) and *meta*-chloroperoxybenzoic acid (*m*-CPBA) were used as oxidants for  $\text{Mn}^{2+}$  catalyzed epoxidation. The full mass spectra and tandem mass spectra using either oxidant were shown in Figure S16. Both PAA and *m*-CPBA reactions produced targeted lipid epoxides and  $\text{Mn}^{2+}$  adducts, however *m*-CPBA reaction generated more side products in the range of  $m/z$  500-650. Therefore, PAA was chosen for the reaction.

Picolinic acid was used as a ligand to conjugate with Mn(II) for catalyzing epoxidation. In the previous work<sup>1</sup>, ligands such as pyrimidinecarboxylic acid, 1-

isoquinolinecarboxylic acid, and 1-methyl-2-imidazolecarboxylic acid were also examined to coordinate with  $Mn^{2+}$  for epoxidation with picolinic acid being the most competent ligand.

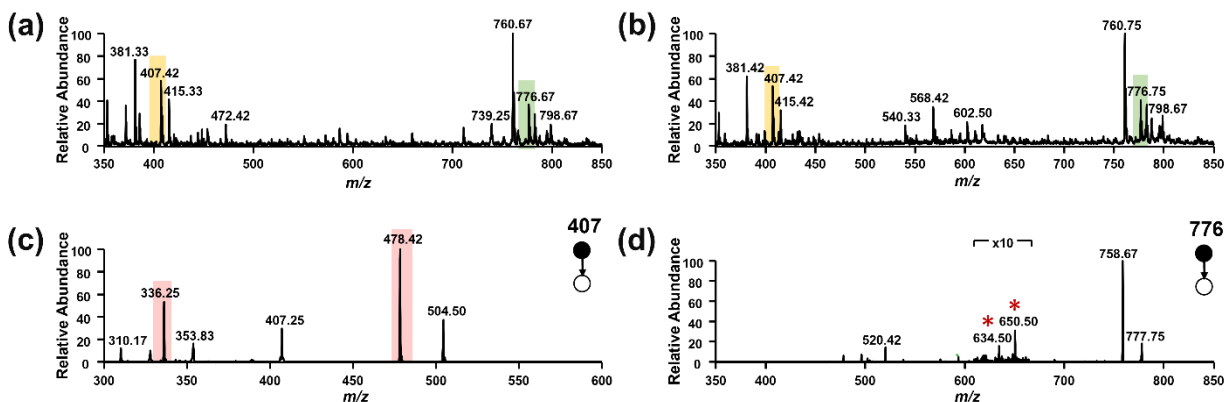


**Figure S16.** Mass spectra after epoxidation of 50  $\mu M$  PC 16:0/18:1(9), 100  $\mu M$   $MnCl_2$ , 1  $\mu M$  picolinic acid and 275  $\mu M$  (a) PAA and (b) *m*-CPBA. CID-MS/MS of (c) *m/z* 407.33 and (d) *m/z* 776.58 in (b).

## S8. Limit of detection

The limit of detection of this method was evaluated with PC 18:1(9)/18:1(9) and PC 16:0/18:1(9). When the concentration of lipid was 5  $\mu M$ , the peaks of native lipids, epoxidized lipids, and Mn-lipid adducts could still be found in full mass spectra, and diagnostic ions could be produced upon CID. When the concentration was 1  $\mu M$ , the peaks of native lipid and epoxidized lipids were hard to see in full spectra, but diagnostic ions could still be observed in tandem mass spectra.

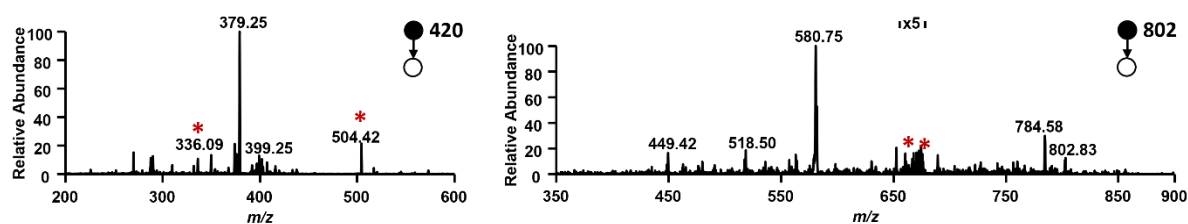


**Figure S17.** Tandem mass spectra of PC 18:1(9)/18:1(9) (1  $\mu M$ ) using PAA (275  $\mu M$ ),  $Mn(CF_3SO_3)_2$  (100  $\mu M$ ) and picolinic acid (1  $\mu M$ ) in ACN.

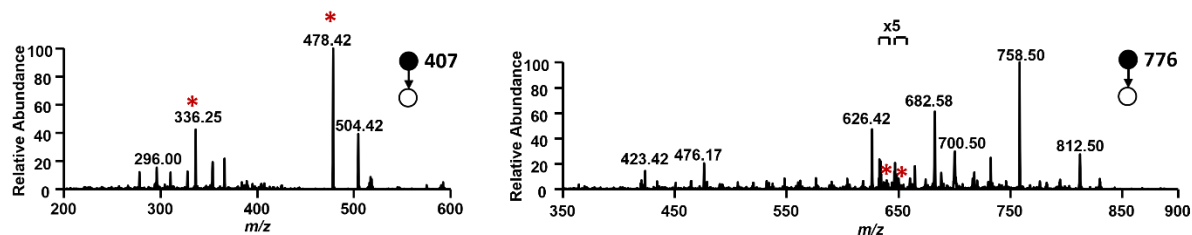


**Figure S18.** Tandem mass spectra of PC 18:1(9)/18:1(9) (1  $\mu$ M) using PAA (275  $\mu$ M),  $\text{Mn}(\text{CF}_3\text{SO}_3)_2$  (100  $\mu$ M) and picolinic acid (1  $\mu$ M) in ACN.

## S9. PLA<sub>2</sub> digestion experiment

The PLA<sub>2</sub> digestion was conducted based on a previous protocol with some modifications.<sup>5</sup> Herein, we prepared a series of lipid solutions consisting of PC 16:0/18:1(9) and PC 18:1(9)/16:0. The molar percentages of PC 18:1(9)/16:0 varied from 0, 20, 40, 60 to 100% at a total lipid concentration of 10  $\mu$ M. The volume of lipid solution was maintained at 2.4 mL, and later sampled into three aliquots of 400  $\mu$ L. One aliquot was mixed with 200  $\mu$ L of aqueous solution containing 20 mM Tris-HCl, 40 mM  $\text{CaCl}_2$ , and 7  $\mu$ g PLA<sub>2</sub>. The mixture was vortexed for 2 min, and incubated at 37  $^\circ\text{C}$  for 4 h afterwards. After the completion of PLA<sub>2</sub> digestion, PC lipids were digested to lyso PC lipids and were then extracted with 500  $\mu$ L of chloroform. The extraction mixture was vortexed for 2 min and centrifuged at 10,000 g for 3 min. The bottom layer was transferred to a vial and dried under nitrogen. The residue was re-suspended in methanol with 1% formic acid for MS analysis.

PC 16:0/18:1(9) was digested to lyso PC 16:0 at  $m/z$  496.34, while PC 18:1(9)/16:0 became lyso PC 18:1(9) at  $m/z$  522.35. The MS ion intensity percentages of the lyso PC lipids PC 18:1(9) and PC 16:0 from PLA<sub>2</sub> digestion (calculated using the ion intensity of  $m/z$  522.35 divided by total ion intensities of  $m/z$  496.34 and 522.35) were plotted against the molar percentages of PC 18:1(9)/16:0 in the *sn*-positional isomer mixtures (Figure S19). A linear relationship with  $R^2 = 0.990$  was obtained. The calibration curve indicates that the *sn*-purity of PC 18:1(9)/16:0 was  $78\% \pm 5\%$ , while the *sn*-purity for PC 16:0/18:1(9) was  $86\% \pm 1\%$ .

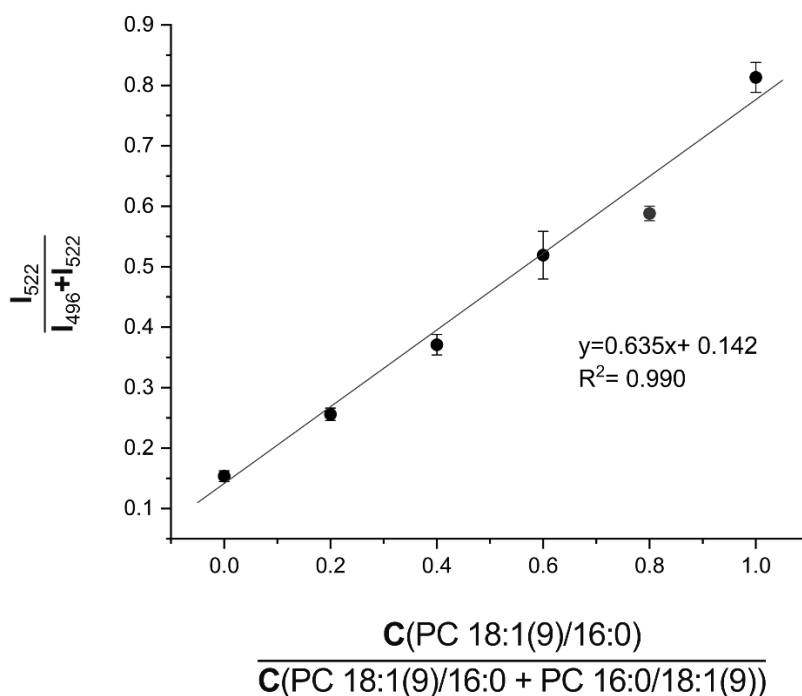


**Figure S19.** Mn adducts with PLA<sub>2</sub> digestion of a series of PC 16:0/18:1 and PC 18:1/16:0 solutions.

### S10. Relative quantification of *sn*-positional isomers

A series of PC 18:1(9)/16:0 and PC 16:0/18:19(9) solutions were used for relative quantification of *sn*-positional isomers. Isolation window widths of 1.0, 1.5, 2.0, 2.5, 3.0 and 3.5 were tested (Figure S20). The intensity of characteristic fragment ions rose, and the linearity of the calibration curve improved with the increase of isolation window width. When the isolation window width was higher than 2.5, good linearity could be achieved.

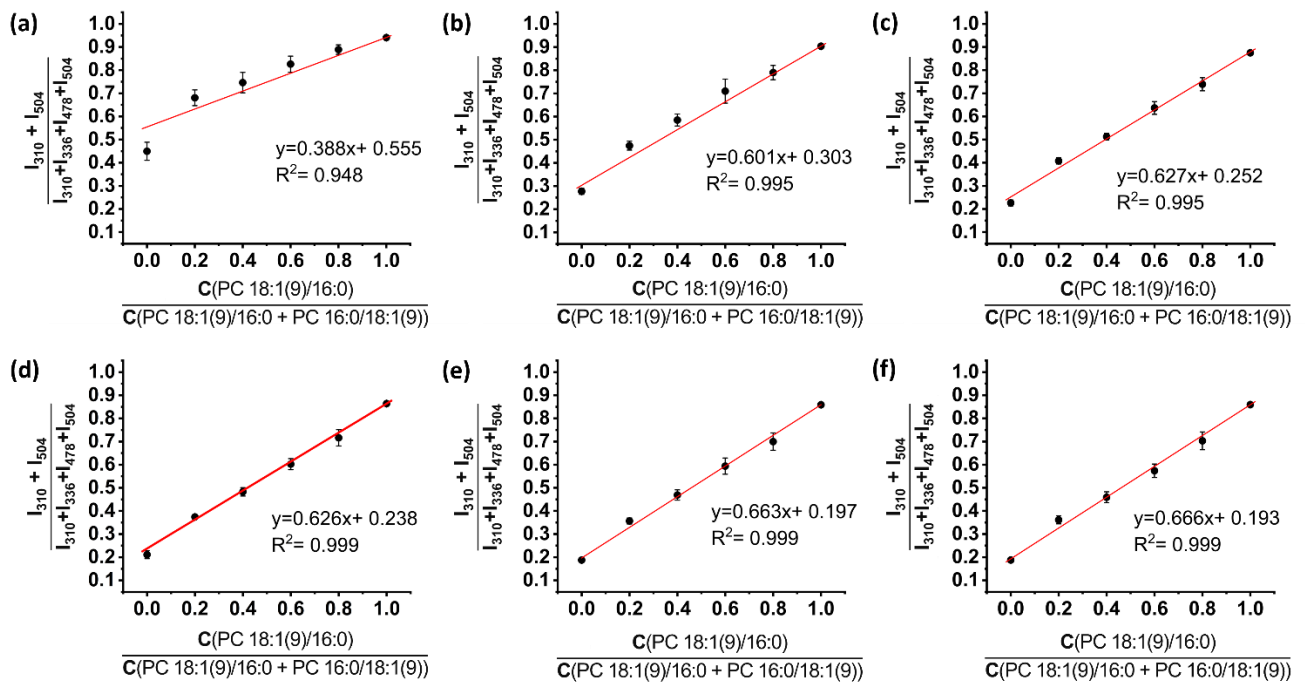


**Figure S20.** Relative quantification curves of *sn*-positional isomers, PC 18:1(9)/16:0 and PC 16:0/18:1(9) with the isolation window widths of (a) 1.0, (b) 1.5, (c) 2.0, (d) 2.5, (e) 3.0 and (f) 3.5 units.

## S11. Lipid isomer identification using lipid extract from egg yolk

### S11.1. Lipid isomer identification in lipid extract from egg yolk

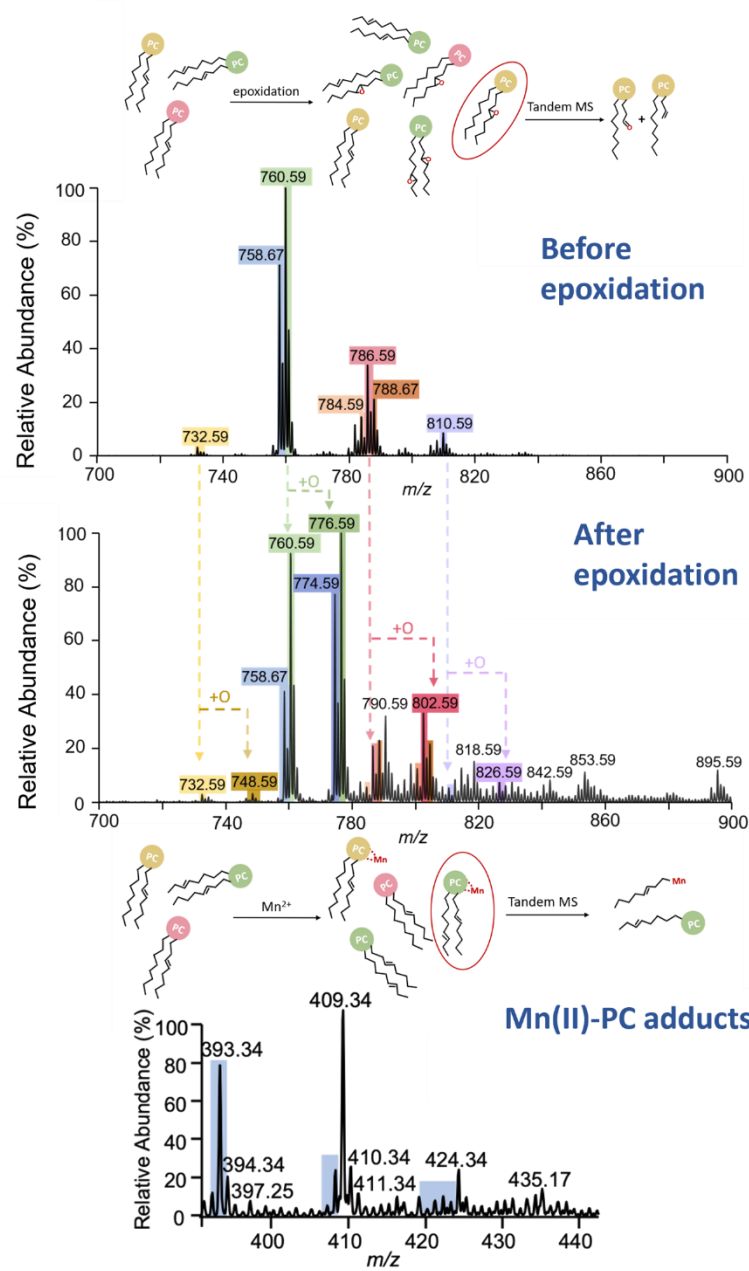
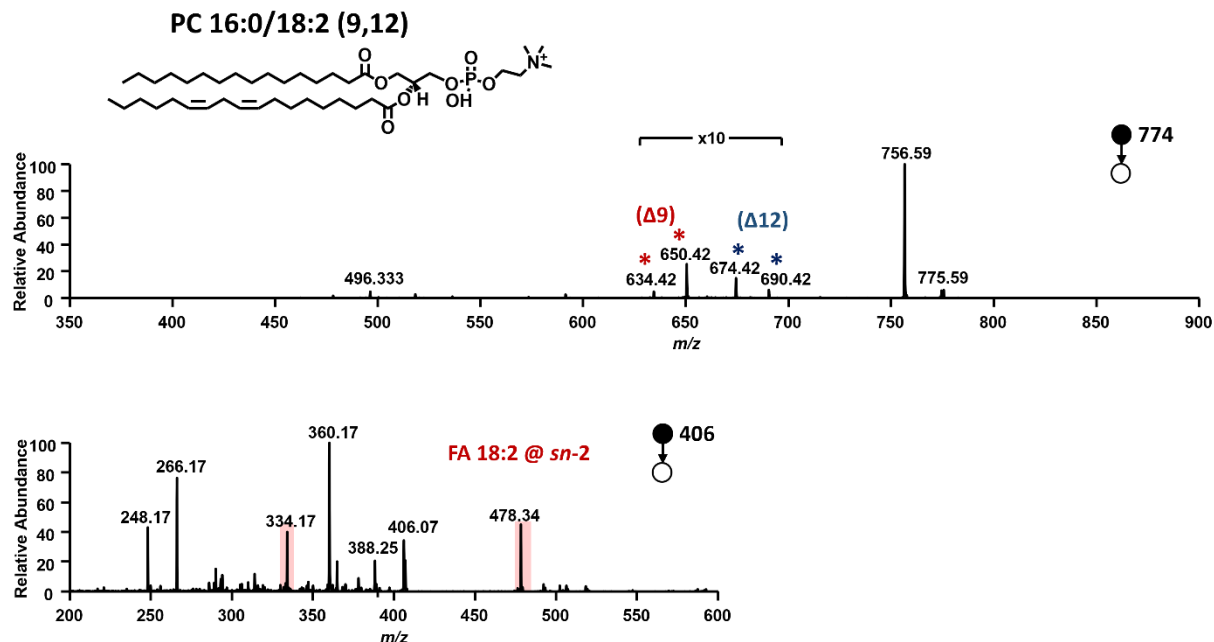


Figure S21. Mass spectra of lipids from egg yolk before and after Mn-catalyzed epoxidation.

**S11.2. An example of C=C bond- and *sn*-positional isomer identification in lipid extract from egg yolk**



**Figure S22.** Tandem mass spectra of epoxidized lipid and Mn-adduct of PC 16:0/18:2 in the lipid extract of egg yolk.

## S12. Comparison of $Mn^{2+}$ catalyzed epoxidation with other methods for lipid isomer identification

Recent development in derivatization-based methodologies prior to mass spectrometric analysis and ion activation methods significantly facilitates lipid isomer identification. We have summarized representative methods in Table S2 which are grouped based on the structural information gained from the method, i.e., (1) C=C bond position identification, (2) *sn*-position identification, and (3) simultaneous C=C bond position and *sn*-position identification. The method developed in this work belongs to the third group. Compared with other methods in this group,  $Mn^{2+}$  catalyzed epoxidation does not require extra instrument apparatus such as an ozone generator, UVPD source, or light source but provides structural information at four lipid isomer levels (i.e., class/subclass, acyl chain length, C=C position, and *sn*-position).

**Table S2.** Representative MS-based methods for lipid isomer identification

Lipid structure information	Method		Lipid scope	Reference
<b>C=C bond position</b>	Chemical derivatization	Methoxylation	FA	Minnikin et al. <i>Chem. Phys. Lipids</i> , 1978
		Cross-metathesis	FA	Kwon et al. <i>Angew. Chem. Int. Ed.</i> , 2011
		Methylthiolation	FAE	Francis et al. <i>Chem. Phys. Lipids</i> , 1981.
		Ozonolysis	FA, GPL, TG, and CE	Brown et al. <i>Biochim. Biophys. Acta</i> , 2011. Hinners et al. <i>Anal. Chem.</i> , 2020.
		<i>m</i> -CPBA epoxidation	FA and GPL	Feng et al. <i>Anal. Chem.</i> , 2019. Kuo et al. <i>Anal. Chem.</i> , 2019.
		PAA epoxidation	FA	Zhang et al. <i>Chem. Sci.</i> , 2021.
		Electrochemical epoxidation	FA	Chintalapudi et al. <i>Chem. Sci.</i> , 2020
		Low-temperature plasma epoxidation	FA and FAE	Zhang et al. <i>Anal. Chem.</i> , 2011.
		Singlet oxygen oxidation	GPL	Unsihuay et al. <i>Angew. Chem. Int. Ed.</i> , 2021
<b>sn Position</b>	Chemical derivatization	(+Fe <sup>2+</sup> ) adduction	PC	Becher et al. <i>Anal. Chem.</i> , 2018.
<b>C=C bond and sn position</b>	Chemical derivatization	PB reaction (+Na <sup>+</sup> or HCO <sub>3</sub> <sup>-</sup> )	C=C bond position for FA, GPL, TG, CE; <i>sn</i> position for PC or GPL	Ma et al. <i>Angew. Chem. Int. Ed.</i> , 2014. Cao et al. <i>Nat. Commun.</i> , 2020.

				Zhao et al. <i>Chem. Sci.</i> , 2019.
		Voltage-controlled electrode epoxidation	<ul style="list-style-type: none"> <li>C=C bond position for FA and GPL; <i>sn</i> position for PC</li> </ul>	Tang et al. <i>Anal. Chem.</i> , 2022.
		Mn-catalyzed epoxidation	<ul style="list-style-type: none"> <li>C=C bond position for FA and GPL; <i>sn</i> position for PC</li> </ul>	<b>This work</b>
	Ion activation	OZID	<ul style="list-style-type: none"> <li>GPL, TG</li> </ul>	Paine et al. <i>Angew. Chem. Int. Ed.</i> , 2018.
		UVPD	<ul style="list-style-type: none"> <li>FA, GPL, cardiolipin, sphingolipid, TG</li> </ul>	Williams et al. <i>J. Am. Chem. Soc.</i> , 2017. Klein et al. <i>Anal. Chem.</i> , 2018.
		EIEIO	<ul style="list-style-type: none"> <li>PC</li> </ul>	Campbell et al. <i>Anal. Chem.</i> , 2015.

Abbreviation of lipids in the table: FA, fatty acid; FAE, fatty acid ester; GPL, glycerophospholipid; TG, triglyceride; CE, cholesterol ester; MSI, mass spectrometry imaging.

## References

1. R. A. Moretti, J. Du Bois and T. D. P. Stack, *Org. Lett.*, 2016, **18**, 2528-2531.
2. Y. Feng, B. Chen, Q. Yu and L. Li, *Anal. Chem.*, 2019, **91**, 1791-1795.
3. H. Zhang, M. Xu, X. Shi, Y. Liu, Z. Li, J. C. Jagodinsky, M. Ma, N. V. Welham, Z. S. Morris and L. Li, *Chem. Sci.*, 2021, **12**, 8115-8122.
4. H. J. Yoo and K. Håkansson, *Anal. Chem.*, 2010, **82**, 6940-6946.
5. W. Cao, S. Cheng, J. Yang, J. Feng, W. Zhang, Z. Li, Q. Chen, Y. Xia, Z. Ouyang and X. Ma, *Nat. Commun.*, 2020, **11**, 375.